Forward and Inverse Analyses of an SMA Actuated Compliant Link

ARTICLE *in* JOURNAL OF MECHANISMS AND ROBOTICS · MAY 2011

Impact Factor: 1.04 · DOI: 10.1115/1.4003528

3 AUTHORS:

Atanu Banerjee

Indian Institute of Technology Guwahati

10 PUBLICATIONS **60** CITATIONS

SEE PROFILE

Bishakh Bhattacharya

Indian Institute of Technology Kanpur

62 PUBLICATIONS **150** CITATIONS

SEE PROFILE

A. K. Mallik

Indian Institute of Engineering Science…

83 PUBLICATIONS **1,085** CITATIONS

SEE PROFILE

Mechanism and Machine Theory 44 (2009) 369–381

Contents lists available at ScienceDirect

Mechanism and Machine Theory

journal homepage: www.elsevier.com/locate/mechmt

Forward and inverse analyses of smart compliant mechanisms for path generation

A. Banerjee *, B. Bhattacharya, A.K. Mallik

Department of Mechanical Engineering, Indian Institute of Technology, C-212, Hall-IV, Kanpur, Uttarpradesh 208016, India

ARTICLE INFO

Article history:
Received 10 August 2007
Accepted 12 March 2008
Available online 23 May 2008

Keywords:
Compliant mechanism
Smart actuators

ABSTRACT

In this paper, an open loop compliant mechanism consisting of two elastic links actuated through piezoelectric actuators has been analyzed. The links may be joined through rigid or elastic hinge connection. The effect of piezoelectric actuators placed on an elastic beam is considered as two concentrated self-balancing moments acting on the beam at the edges of the actuator. Considering the large deflection of the two links of the mechanism under these self-balancing moments as well as end loads, the forward and inverse analyses of the mechanism are carried out. Two numerical schemes, namely, non-linear shooting (NLS) and Adomian decomposition methods (ADM) have been used for solving these problems. Numerical results are included to demonstrate the potential of the proposed methods.

1. Introduction

Compliant mechanisms are composed of elastic links whose deformations are utilized to produce the desired output motion for a given input actuation. Since these are joint-less and monolithic in nature, there is no friction and wear; resulting in improved repeatability, reduced maintenance and simpler manufacturing [1]. But in comparison to a rigid body mechanism, a compliant mechanism yields smaller workspace. Furthermore, large deformation of its links enforces the consideration of geometric and material non-linearity, thus making its design and synthesis a challenging task. Towards the synthesis of compliant mechanisms, two complementary methods are found in the literature: the pseudo-rigid body model [2–4], which utilizes the synthesis technique of rigid body mechanisms and the topology synthesis method [5,6], which uses the structural optimization technique. All these methods are used to design compliant mechanisms for function or path generation tasks. The mechanisms thus produced are mainly of *passive* type, i.e., the sources of input forces and/or moments are not considered in the design. In order to complete the design, proper selection of the actuators is necessary. In this respect, use of smart material actuators is best suited for the actuation of compliant mechanisms because of their wide variety and capability. The combined system of smart material actuators and compliant mechanisms has certain advantages as reported in [7]. These smart material actuated compliant mechanisms can be called *active compliant mechanisms*. But the design and analyses of the resulting smart material actuated compliant mechanisms involve numerous complexities. Besides the requirement of the considerations of geometric and material non-linearity, the input characteristics of the compliant mechanism and the output characteristics of the smart material actuators should also be matched. A theoretical study of such a smart material actuator driven compliant mechanism with the objective of path generation is presented here.

In the literature of compliant mechanisms, mostly closed chain deformable structures are designed or synthesized. The term closed chain mechanism bears the same meaning as in the traditional rigid body mechanism. In this paper, the forward and inverse analyses of an open chain compliant mechanism, consisting of two deformable links joined through a rigid joint

* Corresponding author. Tel.: +91 09450352044.
E-mail address: atanub@iitk.ac.in (A. Banerjee).

0094-114X/$ - see front matter © 2008 Elsevier Ltd. All rights reserved.
doi:10.1016/j.mechmachtheory.2008.03.012

or an elastic hinge and actuated through smart material actuators, have been presented. This mechanism is very similar to a traditional open chain mechanism consisting of rigid links and kinematic pairs, actuated through electric motors or pneumatic drives at each joint. In the present case, the links are elastic and each of them is independently actuated through piezoelectric actuators. The effect of two piezoelectric actuators, mounted on the two opposite sides of an elastic beam and actuated through out of phase voltage, is simulated as two self-balancing moments (equal in magnitude and opposite in sense) acting just at the edge of the actuators. The idealization of replacing a smart patch by two end moments is based on Crawley's model [8,9] of induced strain actuation and is applicable for any smart actuators based on Piezoelectric, Magnetostrictive and Electro-active Polymeric materials. The relation between the applied input voltage to piezoelectric actuators and the output moments exerted by these on the beam is explicitly derived in [9,10]. The stiffness contribution of these smart actuators has been neglected in this analysis. In case of links actuated through multiple actuators, each of them embedded on the surfaces of the beam is replaced by a pair of self-balancing moments, the magnitude of which depend on the applied voltage across the actuator and its material properties. This idea of replacing the piezoelectric actuators with pairs of self-balancing moments has been used in [11]. But in that case, the linear beam theory is used to determine the static deflection. The concept of constructing a flexible mechanism consisting of multiple deformable links, connected in series with rigid or elastic connection and driven through smart material actuators embedded in each of the links, is not found in the literature. Furthermore, there is always an end force and moment acting on the mechanism simulating the payload on the same. This type of flexible mechanisms may be used where precise and repeatable motion is required, such as in cell harvesting.

The present paper is organized in the following manner. First the equilibrium equation of a flexural beam is obtained using Euler–Bernoulli beam theory and the resulting non-linear differential equation is solved using Shooting (NLS) and Adomian decomposition method (ADM). Secondly, the forward analysis (i.e., the determination of the end point trajectory given the actuating moments) has been carried out for the two link flexible mechanism, where the links can be joined through either a rigid or an elastic connection. The actuating moments are distributed over each of the compliant links and for a given range of moments, the workspace has been generated. Finally, the inverse problem (i.e., to determine the moments required to reach the desired points for a given trajectory within the workspace) has been solved.

It should be mentioned that the complete solution of a path generation problem by a smart compliant mechanism must include the dynamics of the actuator and that of the mechanism. However, for low speed actuation and actuators with fast dynamics (e.g., piezoelectric and magnetostrictive actuators) the static analysis discussed in this paper can provide a useful first approximation.

2. Cantilever beam subjected to self-balanced moment and external load

In this section, the large deflection of a cantilever beam under self-balanced moments as well as external force and moment has been formulated and solved.

2.1. Non-linear shooting method for a single link

Fig. 1 shows the deformed shape of a cantilever beam, the model of a compliant segment, subjected to two equal and opposite moments applied at intermediate locations. Furthermore, there is a non-following end force and a moment. The intermediate moments are acting at distances l_1 and l_2 from the fixed end along the length of the deformed beam. The resulting bending moment at any point (x,y) on the beam is given by

$$M_{(x,y)} = P(a-x) + nP(b-y) + M_p[u(s-l_1) - u(s-l_2)] + M_e \tag{1}$$

where s is the distance of the point from the fixed end along the length of the beam, P and nP are the vertical and horizontal components of the non-following end force F, M_p is the moment applied by the actuators, $u(s)$ is the unit step function defined as $u(s) = 0$ for $s < 0$ and $u(s) = 1$ for $s \geqslant 0$ and M_e is the external moment applied at the free end. From Eq. (1) and the Euler–Bernoulli moment–curvature relationship one gets

$$EI\frac{d\theta}{ds} = P(a-x) + nP(b-y) + M_p[u(s-l_1) - u(s-l_2)] + M_e, \tag{2}$$

where $\frac{d\theta}{ds}$ denotes the curvature of the beam and EI is its flexural rigidity. Differentiating Eq. (2) with respect to $\bar{s}$ and substituting $\frac{dx}{ds} = \cos\theta$ and $\frac{dy}{ds} = \sin\theta$ one gets

$$\frac{d^2\theta}{d\bar{s}^2} = -\frac{PL^2}{EI}(\cos\theta + \sin\theta) + \frac{M_pL}{EI}[\delta(\bar{s} - \bar{l}_1) - \delta(\bar{s} - \bar{l}_2)] \tag{3}$$

where $\bar{s} = \frac{s}{L}, \bar{l}_1 = \frac{l_1}{L}, \bar{l}_2 = \frac{l_2}{L}, L$ is the length of the beam and $\delta(s)$ is the Dirac–Delta function defined as $\delta(s) = 0$ for $s \neq 0$ and $\delta(s) \to \infty$ at $s = 0$. Introducing the non-dimensional load parameter $\alpha = \frac{PL^2}{EI}$ and the non-dimensional moment parameter $\kappa = \frac{M_pL}{EI}$ in Eq. (3), one gets

$$\frac{d^2\theta}{d\bar{s}^2} = -\alpha(\cos\theta + \sin\theta) + \kappa[\delta(\bar{s} - \bar{l}_1) - \delta(\bar{s} - \bar{l}_2)]. \tag{4}$$

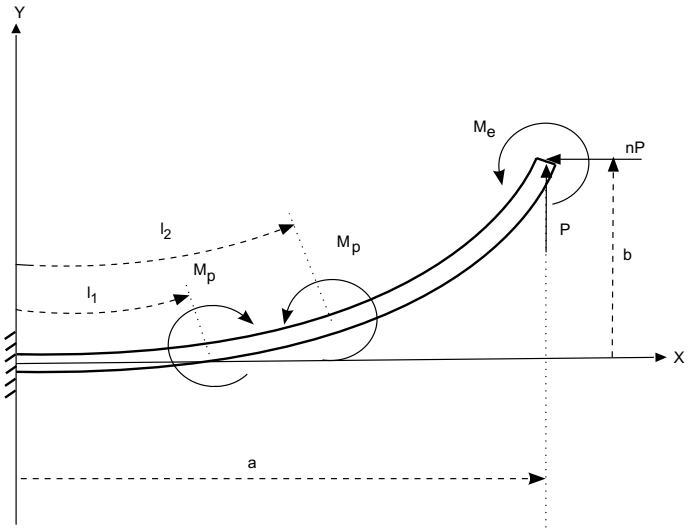

Fig. 1. Deformed shape of an elastic link.

Here, $\delta(\bar{s})$ can be replaced by a sharply rising continuous function such that $\int_{-\infty}^{\infty}\delta(\bar{s})d\bar{s}=1$ is satisfied. This problem is posed as a boundary value problem defined below.

$$\left.\begin{array}{ll}\text{DE} & \frac{d^2\theta}{d\bar{s}^2}=-\alpha(\cos\theta+n\sin\theta)+\kappa[\delta(\bar{s}-\bar{l}_1)-\delta(\bar{s}-\bar{l}_2)]\\ \text{BC} & \begin{cases}\theta|_{\bar{s}=0}=0\\ \frac{d\theta}{d\bar{s}}\big|_{\bar{s}=1}=\tau\end{cases}\end{array}\right\} \tag{5}$$

where $\tau=\frac{M_eL}{EI}$ is the non-dimensional external moment acting at the free end of the beam.

In the NLS method, the boundary value problem (BVP) is converted into an initial value problem (IVP) with an assumed curvature at the fixed end i.e., $c=\frac{d\theta}{d\bar{s}}|_{\bar{s}=0}$. First the differential equation is solved using fourth order Runge–Kutta method with an assumed value of c. Then the value of c is modified till the second boundary condition is satisfied. Here IVP is posed as

$$\left.\begin{array}{ll}\text{DE} & \frac{d^2\theta}{d\bar{s}^2}=-\alpha(\cos\theta+n\sin\theta)+\kappa[\delta(\bar{s}-\bar{l}_1)-\delta(\bar{s}-\bar{l}_2)]\\ \text{BC} & \begin{cases}\theta|_{\bar{s}=0}=0\\ \frac{d\theta}{d\bar{s}}\big|_{\bar{s}=0}=m_k\end{cases}\end{array}\right\} \tag{6}$$

where m_k is assumed to be the curvature at the fixed end at the kth iteration step. Thus, the error involved is determined as error $=\left[\left(\frac{d\theta}{d\bar{s}}\right)_{\bar{s}=1}-\tau\right]$ and this is to be made zero by properly modifying m_k. Newton–Raphson method has been used for this purpose. Here m_k in the kth step is calculated from that of the $(k-1)$th step using

$$m_k=m_{k-1}-\frac{(\text{error})}{\frac{\partial}{\partial m}\left[\frac{d\theta}{d\bar{s}}\big|_{\bar{s}=1}\right]}. \tag{7}$$

Thus, at each step m_k is modified using Eq. (7) till the error is less than some allowable tolerance and finally the solution is achieved. The proof of convergence of this method is explicitly shown in [12]. Obtaining the solution for $\theta(\bar{s}),\bar{x}$ and $\bar{y}$ is obtained using $\frac{d\bar{x}}{d\bar{s}}=\cos\theta$ and $\frac{d\bar{y}}{d\bar{s}}=\sin\theta$, respectively.

For multiple patches, Eq. (5) can be modified as

$$\left.\begin{array}{ll}\text{DE} & \frac{d^2\theta}{d\bar{s}^2}=-\alpha(\cos\theta+n\sin\theta)+\sum\limits_i\kappa_i[\delta(\bar{s}-\bar{l}_1^i)-\delta(\bar{s}-\bar{l}_2^i)]\\ \text{BC} & \begin{cases}\theta|_{\bar{s}=0}=0\\ \frac{d\theta}{d\bar{s}}\big|_{\bar{s}=1}=\tau\end{cases}\end{array}\right\} \tag{8}$$

where i denotes the number of piezo patches and $\bar{l}_1^i$ and $\bar{l}_2^i$ are the distances of the two ends of the ith actuator from the fixed end of the beam. Eq. (8) is used to solve the large deflection beam problem subjected to multiple patches.

Thus, the deformed shape of a single flexible link subjected to multiple pairs of self-balancing moments and end loadings (forces and moments) is obtained using the NLS technique. This method will be iteratively used in modeling the two link flexible mechanism. Issues like obtaining multiple solutions and implementation strategies are elaborately discussed in [13].

2.2. Adomian decomposition method for a single link

ADM provides an analytical solution to non-linear ordinary and partial differential equations in series form. The method has been used to solve numerous engineering and scientific problems governed by non-linear ordinary and partial differential equations [14–18]. The non-linear terms in the governing differential equation are decomposed into polynomials using Taylor's series, known as Adomian polynomials, and are used to obtain the analytical solution. The method and its proof of convergence have been elaborately explained in [19–22].

Our aim is to solve the boundary value problem governed by the non-linear differential equation given by Eq. (4). Integrating Eq. (4) twice with respect to $\bar{s}$, using the BCs' and upon simplification, the governing equation takes the form

$$\left.\begin{aligned}
\theta_1(\bar{s}) &= c\bar{s} + \alpha\int_0^{\bar{s}}\int_0^{t}(\cos\theta + n\sin\theta)\mathrm{d}\bar{s}\,\mathrm{d}t && \text{for } 0 \leqslant \bar{s} < \bar{l}_1\\
\theta_2(\bar{s}) &= c\bar{s} + \alpha\int_0^{\bar{s}}\int_0^{t}(\cos\theta + n\sin\theta)\mathrm{d}\bar{s}\,\mathrm{d}t + \kappa(\bar{s}-\bar{l}) && \text{for } \bar{l}_1 \leqslant \bar{s} < \bar{l}_2\\
\theta_3(\bar{s}) &= c\bar{s} + \alpha\int_0^{\bar{s}}\int_0^{t}(\cos\theta + n\sin\theta)\mathrm{d}\bar{s}\,\mathrm{d}t + \kappa(\bar{l}_2-\bar{l}_1) && \text{for } \bar{l}_2 \leqslant \bar{s} < 1
\end{aligned}\right\} \tag{9}$$

where $c = \frac{\mathrm{d}\theta}{\mathrm{d}\bar{s}}\big|_{\bar{s}=0}$. $\theta_1(\bar{s})$, $\theta_2(\bar{s})$ and $\theta_3(\bar{s})$ are, respectively, the angle that the tangent at any point on the three segments of the beam makes with the X-axis. Each of the integral equations is solved by expanding the non-linear term within the integral using Adomian polynomials about $\theta_{\bar{s}=0} = 0$. The procedures to obtain the coefficients of Adomian polynomials corresponding to a particular non-linear term are explicitly explained in [13,18].

Unlike the NLS, the unknown c, is determined by satisfying the moment boundary condition specified at the free end i.e., $\frac{\mathrm{d}\theta}{\mathrm{d}\bar{s}}\big|_{\bar{s}=1} = \tau$. Once $\theta(\bar{s})$ is obtained for each of the segments, $(\bar{x}(\bar{s}), \bar{y}(\bar{s}))$ can be computed using $\frac{\mathrm{d}\bar{x}}{\mathrm{d}\bar{s}} = \cos\theta$ and $\frac{\mathrm{d}\bar{y}}{\mathrm{d}\bar{s}} = \sin\theta$. This can be done either by expanding the sine and cosine terms in Taylor's series or by numerical integration. Since the Adomian polynomial used in approximating the non-linear term in Eq. (9) is truncated, the corresponding solution is not exact and thus c^0 continuity will not be maintained in between the segments. In order to enforce the continuity, the errors i.e. $(\theta_1 - \theta_2)$ at $\bar{s} = \bar{l}_1$ and $(\theta_2 - \theta_3)$ at $\bar{s} = \bar{l}_2$ are deducted from $\theta_2(\bar{s})$ and $\theta_3(\bar{s})$, respectively. Thus the entire beam configuration is obtained.

This procedure can be extended for a beam with multiple patches also, where the number of equations increases accordingly. For each additional actuator two new equations are to be solved.

Thus, ADM can be used to obtain the deformed shape of a single piece flexible link subjected to multiple pairs of self-balancing moments as well as end loadings. In the next section, this method has been iteratively used to solve the two link mechanism problem. Implementation strategy and convergence issues have been thoroughly discussed in [13].

3. Forward analysis of a two link mechanism

The objective of the forward analysis is to determine the position of the end point of the mechanism for given actuating moments M_p^is' applied by the actuators while manipulating an external load at the end.

3.1. Non-linear shooting method

The method elucidated in Section 2.1 for a single elastic link and multiple patches is iteratively used to solve the two link mechanism problem. The equilibrium of each link is considered separately under all the external forces and moments as well as the mutual reactions between the neighboring links. The algorithm is shown step by step in the next section. All the symbols have been defined in previous sections.

3.1.1. Two link flexible mechanism with rigid connection

Fig. 2 shows a flexible mechanism consisting of two elastic links connected rigidly. The angle between the links is β. Each of the links is of length L and actuated through a pair of self-balancing moments M_p^1 and M_p^2, respectively. The components of the non-following force P and nP and the moment at the free end M_e are simulating a non-following payload. The free body diagram of each of the elastic links is shown in Fig. 3. Here M_x is the reaction moment acting between the links. Two coordinate systems are depicted in this figure. The coordinate system (X,Y) is the fixed reference, with its abscissa along the undeflected axis of the link-I. The final coordinates of the end points (X_1, Y_1) and (X_2, Y_2) of link-I and link-II, respectively, have been defined in this coordinate system. The (x,y) coordinate system with its origin at the end of link-I and its abscissa along the undeflected axis of the link-II has been used to write the equilibrium equation of the second link. The algorithm for solving the forward analysis is as follows:

Step I: The normalized end force α and moment τ are determined for a given payload using the normalization scheme described above.

Step II: Configuration of the link-I is obtained using α, n, κ_1 and τ_x, where $\kappa_1 = \frac{M_p^1 L}{EI}$, the normalized actuating moment on the link-I and $\tau_x = \frac{M_x L}{EI}$, the normalized end moment, which is initially assumed to be zero.

Step III: Configuration of link-II is determined corresponding to α', n', κ_2 and τ, where α' and n' are obtained by transforming the end forces in the coordinate system (x,y) (obtained through rotation of the original reference (X,Y) by an angle equal to $(\theta_e - \beta)$); where θ_e is the angle that the tangent drawn at the end of link-I makes with the X-axis, $\kappa_2 = \frac{M_p^2 L}{EI}$ is

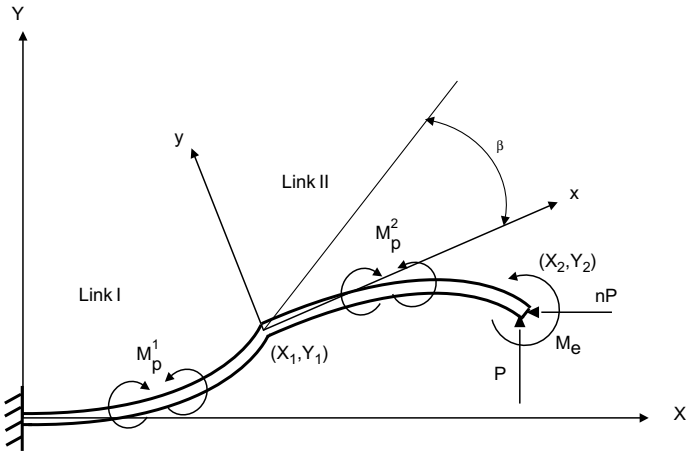

Fig. 2. Deformed two-link flexible mechanism.

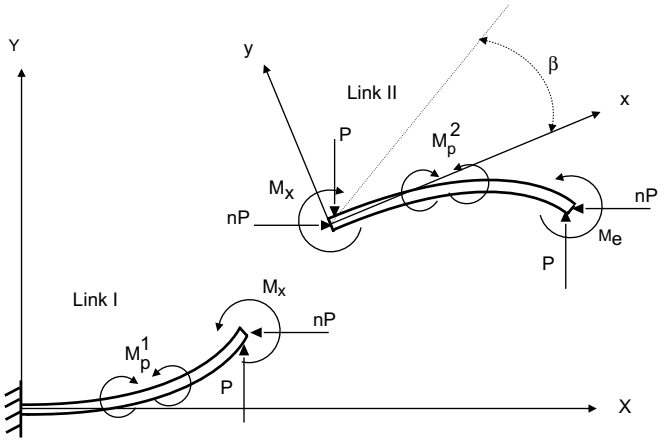

Fig. 3. Free body diagram of two elastic links connected through rigid joints.

the normalized actuating moment on link-II and $\tau = \frac{M_e L}{EI}$ is the normalized end moment. Since the joint is rigid, angle β remains unchanged even after deformation of the links.

Step IV: From the final configuration of the link-II, the normalized moment τ_x at the end of link-I which is equal and opposite to the moment at the beginning of link-II is computed using

$$\tau_x = \alpha(\overline{X}_2 - \overline{X}_1) + n\alpha(\overline{Y}_2 - \overline{Y}_1) \tag{10}$$

where $\overline{X} = \frac{X}{L}$ and $\overline{Y} = \frac{Y}{L}$.

Step V: The non-zero value of τ_x, the non-dimensional moment applied by link-II on link-I, yield a new configuration of link-I and simultaneously changes the position and orientation of the (x,y) axes and thus yields new values of α', n'. In this way a new configuration of link-II is obtained.

Step VI: Again the value of the normalized reaction moment τ_x is updated and the deformed configuration for link-I is computed, resulting in a new value of θ_e.

Step VII: The procedures described in step III to step VI are continued until and unless the difference in the old and the new value of τ_x is less than the allowable tolerance.

The convergence in the value of τ_x means both the links are in equilibrium under the action of the actuating moments κ_1 and κ_2 as well as the end force α and the end moment τ.

3.1.2. Two link flexible mechanism with elastic hinge connection

The free body diagrams of the two links as well as that of the hinge are shown in Fig. 4. In the undeformed condition of the hinge, the angle between the links is β, and ψ is the change in the value of β i.e., the angular deformation of the hinge. The coordinate systems and the rest of the symbols remain same as defined in the previous section. In this case, apart from the

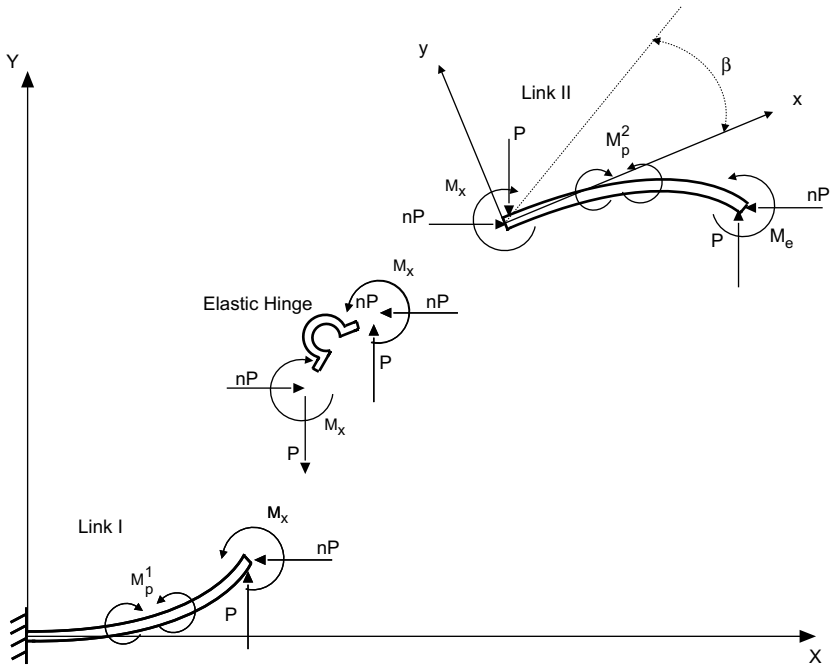

Fig. 4. Free body diagram of two elastic links and elastic hinge.

equilibrium of the links, the equilibrium of the hinge is also to be considered. The steps of the solution algorithm are detailed below.

Steps I and II remain the same as in Section 3.1.1. In step III, the end forces (α', n') are obtained by rotating the coordinate (X, Y) by an angle $(\theta_e - \beta - \psi)$ instead of $(\theta_e - \beta)$, where ψ (equal to the change in β) is the angular deflection of the elastic hinge connecting the two links. Following step IV described in the previous section the normalized end moment τ_x is calculated. Since τ_x is known, ψ, the angular deflection of the elastic hinge is determined using the relation $\tau_x = \varsigma\psi$, where ς is the normalized stiffness of the elastic hinge. If K_ψ is the angular stiffness of the hinge, the normalized stiffness is obtained using $\varsigma = \frac{K_\psi L}{EI}$, where EI is the flexural rigidity and L is the length of each link. It may be considered as the relative stiffness of the hinge with respect to the links. In each iteration the value of ψ is computed and incorporated for the transformation of the end forces from (X, Y) coordinate system to (x, y) coordinate system. Rests of the steps are same as in the case of elastic links with rigid connection reported in Section 3.1.1.

3.2. Adomian decomposition method

The ADM discussed in Section 2.2 provides a closed form solution of Eq. (9) i.e., for $\theta(\bar{s})$ of a single link. Those solutions are used iteratively to solve the two link mechanism problem just as in the case of NLS method. The details of the steps are listed below.

3.2.1. Two link flexible mechanism with rigid connection

Step I: Using the expression of $\theta(\bar{s})$ for link-I obtained in Section 2.2, the unknown $c = \frac{d\theta}{d\bar{s}}|_{\bar{s}=0}$ is determined with the initial assumption of $\tau_x = 0$. Thus the deformed shape of link-I and hence θ_e is determined.

Step II: The end force parameters (α', n') are determined by transforming (α, n) from (X, Y) coordinate system to (x, y) coordinate system. The transformation involves the rotation of (X, Y) axes by an amount $(\theta_e - \beta)$. Since the connection is rigid, β remains unchanged.

Step III: The values of (α', n') and the end moment τ are utilized to compute the second link configuration. In this case, c for the link-II is determined using the expressions for $\theta(\bar{s})$ and $\frac{d\theta}{d\bar{s}}|_{\bar{s}=1} = \tau$.

Step IV: Resulting $(\overline{X}_2, \overline{Y}_2)$ leads to a non-zero value of τ_x, calculated using Eq. (10). Consequently the end slope of link-I and in turn the values of $(\overline{X}_2, \overline{Y}_2)$ are changed.

Step V: Steps I–IV are continued till the difference in the old and new τ_x is less than an allowable value.

3.2.2. Two link flexible mechanism with elastic hinge connection

In this case, all the steps except the third one discussed in Section 3.2.1 remain same. Since the hinge is deformable, the angle β between the two elastic links no longer remains unaltered. Thus, the coordinate transformation of the end forces

from (X,Y) to (x,y) is obtained through the rotation of the reference coordinate (X,Y) by an angle $(\theta_e - \beta - \psi)$ as is done in Section 3.1.2.

4. Inverse analysis of a two link mechanism

The objective of the inverse analysis is to determine the actuating moments M_p required in each of the links to guide the end point of the mechanism through some desired locations. Though both the methods described above are capable of handling multiple actuators, only one actuator at each of the link is considered.

Both the NLS and ADM can be used for this analysis. The latter method becomes computationally intensive with increasing load parameters as discussed in [13]. But the effectiveness and the accuracy of the former remains independent of the magnitude of the force parameters. Hence in this work, the NLS method is used for the inverse analysis. But for low values of load parameters, ADM may be advantageous. In any case, the idea of solving the inverse problem is same for both the methods. For a given end loading, the workspace increases considerably with an elastic connection between the links. In order to reduce the size of the workspace, only the rigid connection between the links has been considered for the inverse problem.

4.1. Inverse analysis using shooting method

As discussed in Section 3.1.1, the end point (X_2,Y_2) of the two link mechanism with rigid connections, is a function of the self-balanced moments (M_p^1, M_p^2) and the end forces and moment (P,n,M_e). This can be represented as

$$\left.\begin{aligned} X_2 &= \phi_1(M_p^1, M_p^2, P, n, M_e) \\ Y_2 &= \phi_2(M_p^1, M_p^2, P, n, M_e) \end{aligned}\right\} \tag{11}$$

While using one actuator in each of the links, two unknowns M_p^1 and M_p^2 are to be solved from the two equations given by Eq. (11). Hence the system is consistent and this is one of the reasons for choosing one actuator in each link.

Use of multiple actuators will definitely increase the size of the workspace as well as the manipulators capability to trace more and more complex trajectories. But in that case, the number of unknowns is greater than the number of equations and thus optimization schemes might result in multiple solutions.

5. Results and discussion

Fig. 5a shows the deformed cantilever beam configurations obtained by using both NLS and ADM. The center of the piezo actuators are assumed to be at a distance of 25% and 45% of the beam length measured from the fixed end. The normalized actuating moments κ_is′ are varied while the normalized end force parameters α and the end moment τ are kept constant. In Fig. 5b, κ_is' are kept constant while the end load parameters are varied. The occurrence of inflection points, depending on the combinations of α and τ, may be noted in Fig. 5b. Thus it is confirmed that both these methods, unlike the elliptic integral method [3,4], can handle inflection point without any special treatment.

Fig. 5c shows the path generated by the free end (X_1,Y_1) of the cantilever, as each actuator, placed at different locations, applies a moment κ varying from -1 to +1 in steps of 0.1. It is clearly seen that, by using a single link, the shape of the end point trajectory does not significantly alter by changing the location of the actuator. Furthermore, the movement along the X-axis is also insignificant. This calls for the necessity of using a two link mechanism to generate a complicated trajectory.

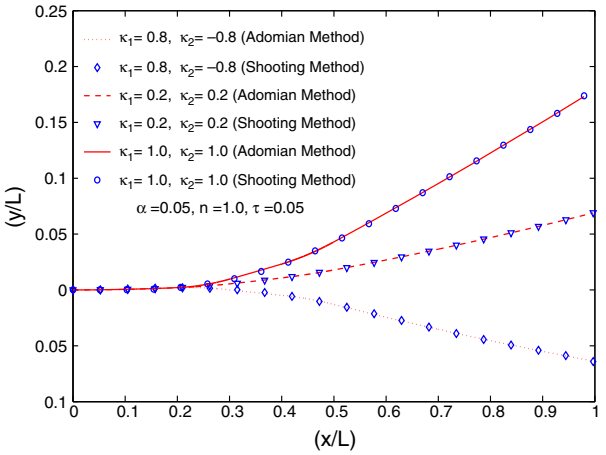

Fig. 5a. Deformed configurations of a single link with different actuating moment and constant end load.

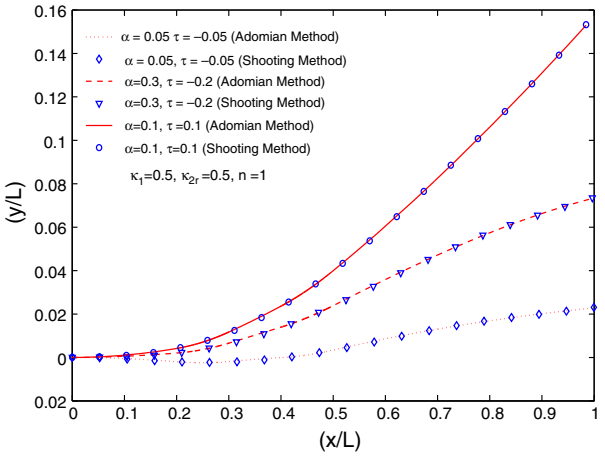

Fig. 5b. Deformed configurations of a single link with different end load and constant actuating moment..

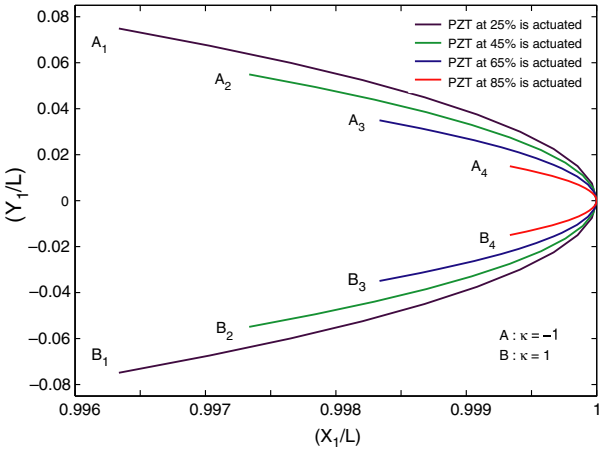

Fig. 5c. Path generated by a single link mechanism.

Fig. 6a shows the deformed configurations of a two link mechanism connected through a rigid joint for various actuating moments and constant end load parameters. Both ADM and NLS method yield the same results. In this case the angle (β) between the two links is taken as 90°. Here, each of the links is embedded with one piezo actuator, i.e., two self-balancing

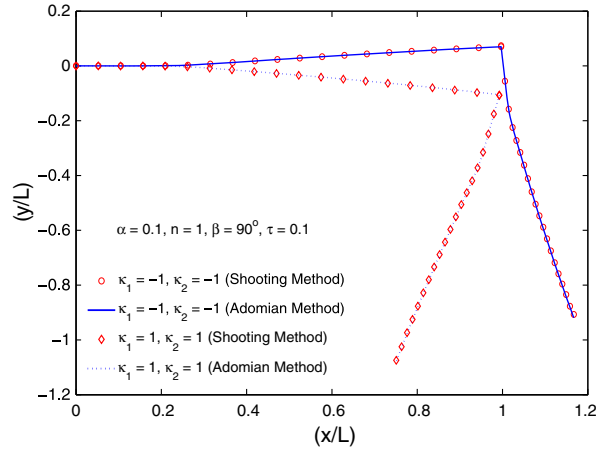

Fig. 6a. Deformed configurations of a two link mechanism with rigid connection with different actuating moment.

moments are acting on each link. Fig. 6b exhibits the deformed mechanism shape for constant actuating moments with varied end moments. For constant actuating moments and end loading conditions the effect of the angle β on the deformed shape of the mechanism can be seen in Fig. 6c.

The deformed configurations when the links are joined through an elastic hinge (of given stiffness) are shown in Fig. 6d for various loading combinations. Comparing Figs. 6b and 6d it can be observed that, the mechanism consisting of an elastic hinge ($\varsigma = 1$, as in Fig. 6d) undergoes larger deflection than that with a rigid joint ($\varsigma = \infty$, as in Fig. 6b). In order to see the effect of hinge stiffness, the mechanism configurations are plotted for various stiffness values of the hinge in Fig. 6e. These results are computed using only the NLS method. Obviously the results tend to that with a rigid joint, as ς increases.

Every mechanism has its own working area, within which it is designed to manipulate the payload. In case of path generation with precision points approach, the end point of the mechanism is desired to go through the accuracy points located on the prescribed path. These accuracy points are chosen in advance to generate the prescribed path. In order to have an idea of all these, the workspace of the mechanism has been generated with the full capacity of the actuators as well as the payload for which it is to be designed. A sample workspace is shown in Fig. 6f. The workspace of the two link mechanism with a rigid connection is computed using NLS method by varying κ_1 and κ_2 from -1 to 1 for $\alpha = 0.1$, $n = 1$ and $\beta = 90°$.

As mentioned earlier, only the NLS method is used for inverse analysis, because of its effectiveness in computation. ADM can also be used for inverse analysis, but the range of load parameters is limited in order to obtain desired accuracy with reasonable computational effort. Fig. 7a shows the generation of a straight line with seven accuracy points. First, the actuating moments are computed by the inverse analysis for a given accuracy point. Thereafter, the actuating moments are used in the forward analysis to obtain the points actually reached. The maximum error, defined as the distance between the target accuracy point and the point reached, is in the order of 10^{-6} times the link length. The actuating moments κ_is' required to

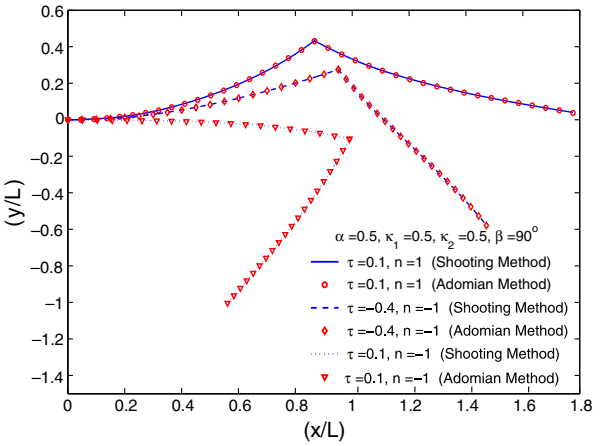

Fig. 6b. Deformed configurations of a two link mechanism with rigid connection with different end load.

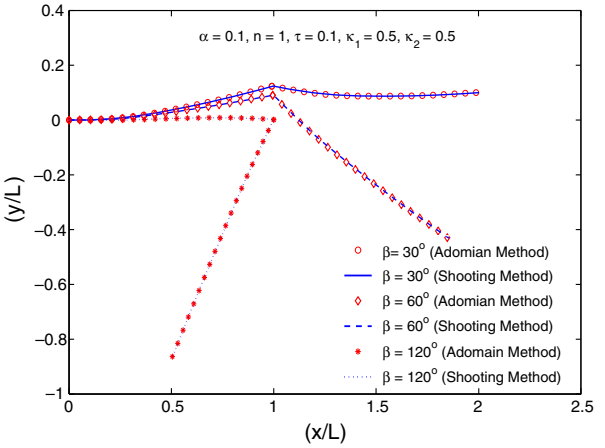

Fig. 6c. Deformed configurations of a two link mechanism with rigid connection with different angle between the links.

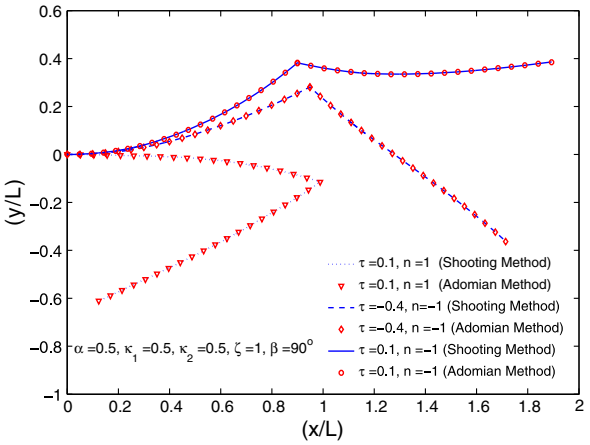

Fig. 6d. Deformed configurations of a two link mechanism with elastic hinge.

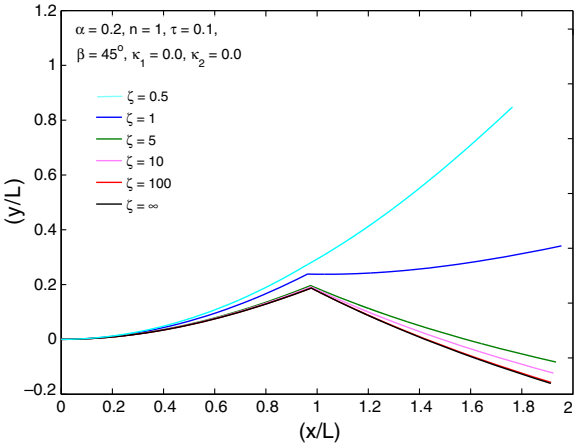

Fig. 6e. Deformed configurations of a two link mechanism for various hinge stiffness.

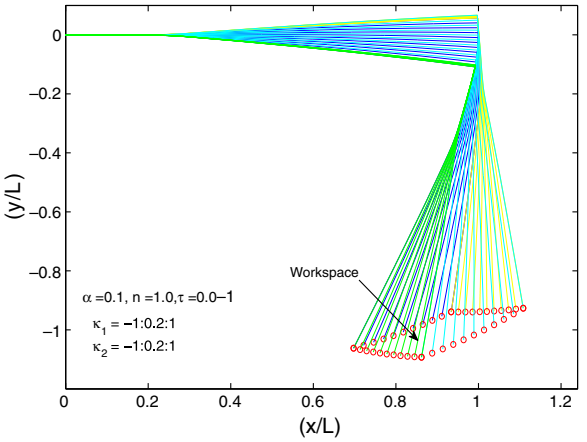

Fig. 6f. Workspace of a two link mechanism with rigid connection.

generate the straight line in Fig. 7a are shown in Fig. 7b. This shows that a gradual change in moments (i.e., the voltage applied to the piezo) is required for each of the PZT actuators. Similar results for generating a circular path and a figure of eight are shown in Figs. 7c–7f.

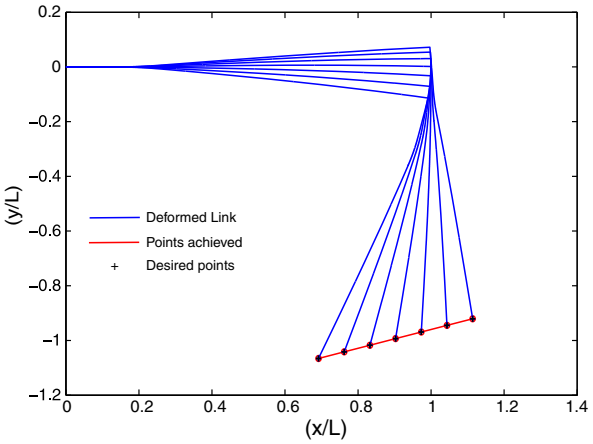

Fig. 7a. A two link mechanism tracing a straight line.

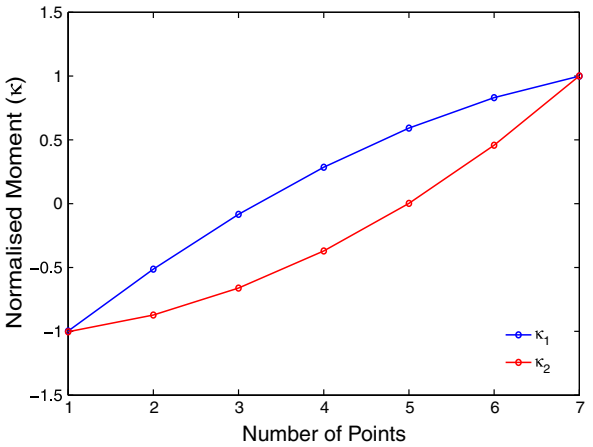

Fig. 7b. Normalized moments required to trace the straight line.

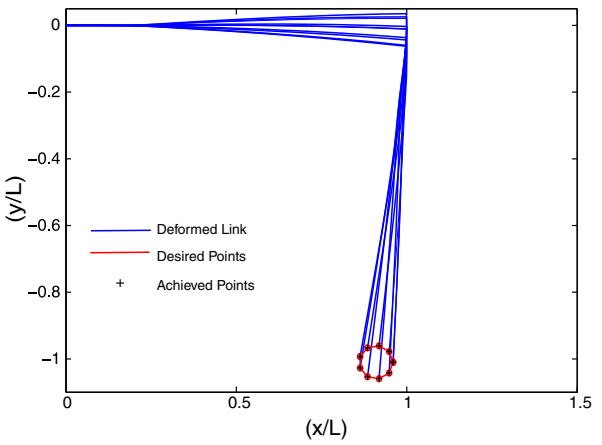

Fig. 7c. A two link mechanism tracing a circle.

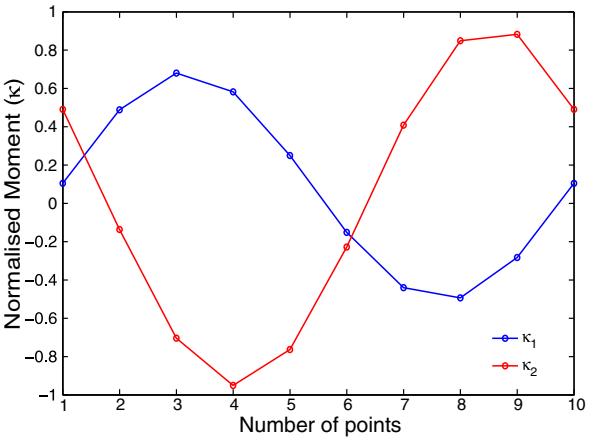

Fig. 7d. Normalized moments required to trace the circle.

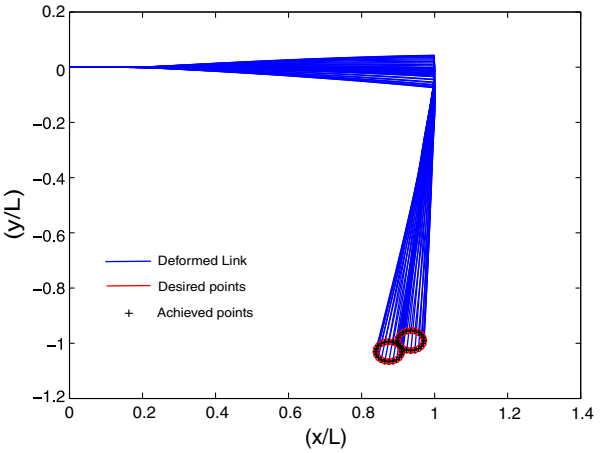

Fig. 7e. A two link mechanism tracing a figure of '8'.

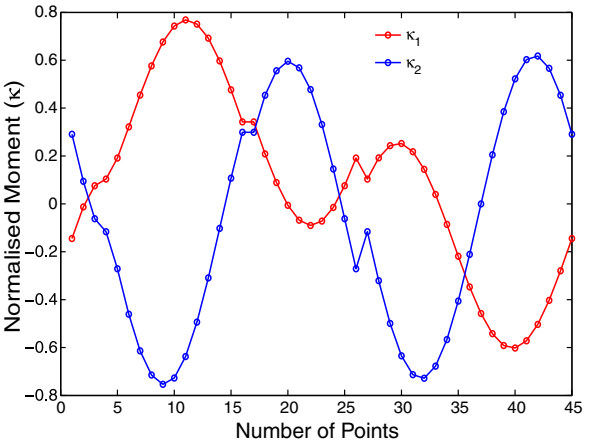

Fig. 7f. Normalized moments required to trace the figure of '8'.

6. Conclusions

A forward and an inverse analysis of path generation by a two link flexible mechanism actuated through smart actuators are presented. Two different methods viz., the non-linear shooting (NLS) and Adomian decomposition methods (ADM) have been used. The methods are proved to be versatile for a range of loading parameters which may or may not cause inflection points within a link. Numerical results are included with different trajectories, viz., a straight line, a circle and a figure of eight.

In future these algorithms will be extended for forward and inverse analyses of closed chain fully compliant mechanisms.

Acknowledgements

The authors gratefully acknowledge the support provided for this research by the Department of Science and Technology (DST) of India under the Grant DST-2006-0263.

References

[1] T.E. Shoup, C.W. McLarnan, A survey of flexible link mechanism having lower pairs, J. Mech. 6 (3) (1971) 97–105.
[2] L.L. Howell, A. Midha, A method for the design of compliant mechanisms with small length flexural pivots, ASME J. Mech. Des. 116 (1) (1994) 280–290.
[3] L.L. Howell, A. Midha, Parametric deflection approximations for end-loaded large deflection beams in compliant mechanisms, ASME J. Mech. Des. 117 (1) (1995) 156–165.
[4] C. Kimball, L.-W. Tsai, Modeling of flexural beams subjected to arbitrary end loads, ASME J. Mech. Des. 124 (2) (2002) 223–234.
[5] A. Saxena, G.K. Ananthasuresh, Topology synthesis of compliant mechanisms for non-linear force-deflection and curved path specifications, ASME J. Mech. Des. 123 (1) (2001) 33–42.
[6] D. Xu, G.K. Anathasuresh, Freeform skeletal shape optimization of compliant mechanisms, ASME J. Mech. Des. 125 (2) (2003) 253–261.
[7] <http://www.flxsys.com/>.
[8] E.F. Crawley, J. Luis, Use of piezoelectric actuators as elements of intelligent structures, AIAA J. 25 (10) (1987) 1373–1385.
[9] E.F. Crawley, Intelligent structures for aerospace: a technology overview and assessment, AIAA J. 32 (8) (1994) 1689–1699.
[10] S.O. Reza Moheimani, A.J. Flemming, Piezoelectric Transducers for Vibration Control and Damping, Springer, Germany, 2006.
[11] P. Gaudenzi, R. Barboni, Static adjustment of beam deflections by means of induced strain actuators, Smart Mater. Struc. 8 (2) (1999) 278–283.
[12] A. Stanoyevitch, Introduction to Numerical Ordinary and Partial Differential Equations Using Matlab, John Wiley and Sons Inc., New Jersey, 2005.
[13] A. Banerjee, B. Bhattacharya, A.K. Mallik, Large deflection of cantilever beams with geometric nonlinearity: numerical and analytical approaches, Int. J. Non-linear Mech (in press).
[14] G. Adomian, Solving Frontier Problems of Physics: The Decomposition Method, Kluwer, Boston, 1994.
[15] A. Wazwaz, A reliable algorithm for solving boundary value problems for higher-order integro-differential equations, Appl. Math. Comput. 118 (2) (2001) 327–342.
[16] I. Hashim, Adomian decomposition method for solving boundary value problems for fourth-order integro-differential equations, J. Comput. Appl. Math. 193 (2) (2006).
[17] V. Seng, K. Abbaoui, Y. Cherruault, Adomian's polynomials for non-linear operators, Math. Comput. Model. 24 (1) (1996) 59–65.
[18] A. Wazwaz, A new method for calculating Adomian polynomials for non-linear operators, Appl. Math. Comput. 111 (1) (2000) 33–51.
[19] Y. Cherruault, Convergence of Adomian method, Math. Comput. model. 14 (1) (1990) 83–86.
[20] Y. Cherruault, G. Saccomandi, B. Some, New results for convergence of Adomian's method applied to integral equations, Math. Comput. Model. 16 (2) (1992) 85–93.
[21] Y. Cherruault, G. Adomian, Decomposition method: a new proof of convergence, Math. Comput. Model. 18 (12) (1993) 103–106.
[22] K. Abbaoui, Y. Cherruault, Convergence of Adomian method applied to non-linear equations, Math. Comput. Model. 20 (9) (1994) 69–73.